Table I

	Method	Hfs and spin densities 1	2	3	4	5	6
Cyclohexadienyl 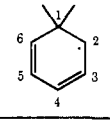	Expt	47.5 0.095	10.4 0.358	2.5 −0.088	10.4 0.358	2.5 −0.088	10.4 0.358
	Theory	47.5 0.095	10.4 0.358	2.6 −0.093	10.6 0.373	2.6 −0.093	10.4 0.358

	Method	Hfs and spin densities 1	2	3	4	5	6	7	8
Naphthyl 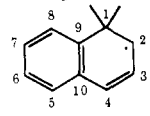	Expt	37 0.074	12.8 0.450	...	12.8 0.450	...	...	...	...
	Theory	37 0.074	12.9 0.454	3.1 −0.110	11.8 0.415	2.5 0.088	0.7 −0.02	2.2 0.076	0.5 −0.014

In the case of toluene and the xylenes, however, the spin density on the sp^3 carbon agreed fairly well with the experimental values.

Acknowledgment. The authors wish to thank Dr. Roman Sioda and Mr. Garrett Odell for programming the McLachlan calculations on the IBM 7094.

Paramagnetic Absorption of Irradiated Glycine[1]

Harold C. Box, Harold G. Freund, and Edwin E. Budzinski

Contribution from the Biophysics Department, Roswell Park Memorial Institute, Buffalo, New York. *Received September 15, 1965*

Abstract: Single crystals of deuterated glycine, $^+ND_3-CH_2-COO,^-$ were irradiated at 77°K and subsequently warmed to 165°K. Well-defined electron spin resonance spectra were observed due to either CH_2COO^- or CH_2COOD. The intensities of sixteen allowed and "forbidden" transitions calculated on the basis of a simple model agree well with the observed hyperfine patterns.

The use of electron spin resonance (esr) spectroscopy for the study of radiation damage in organic materials began about 11 years ago.[2] Probably the most thoroughly investigated organic material to date has been irradiated glycine which crystallizes as the zwitterion $NH_3^+CH_2COO^-$. The room-temperature absorption pattern of X-irradiated glycine is complicated by the presence of more than one kind of free radical. The absorption has been variously assigned to the free radicals $CH_2NH_3^+$, $CH_3CO_2^-$, NH_2, NH_4, and $NH_3^+CHCO_2^-$.[2-4]

In this investigation low temperature was used to stabilize an earlier phase of the radiation damage process. Single crystals of glycine were irradiated at low temperature, subsequently warmed to a prescribed temperature, and studied by esr spectroscopy. Unlike the room temperature absorption, the observed spectra were definitive for all orientations of the crystals.

(1) Supported in part by Public Health Service Grant GM10873 and Atomic Energy Commission Contract AT(30-1)3558.

(2) J. Combrisson and J. Uebersfeld, *Compt. Rend.*, **238**, 1397 (1954).

(3) W. Gordy, W. B. Ard, and H. Shields, *Proc. Natl. Acad. Sci. U. S.*, 41, 983 (1955); J. Uebersfeld and E. Erb. *Compt. Rend.*, **242**, 478 (1956); M. C. R. Symons, *J. Chem. Soc.*, 277 (1959); D. K. Ghosh and D. H. Whiffen, *Mol. Phys.*, **2**, 285 (1959); *J. Chem. Soc.*, 1869 (1960).

(4) R. F. Weiner and W. S. Koski, *J. Am. Chem. Soc.*, **85**, 873 (1963); J. R. Morton, *ibid.*, **86**, 2325 (1964).

Experimental Method

Monoclinic crystals of glycine were grown by slow evaporation of aqueous solution. The crystals belong to the space group $P2_1/n$ with four molecules per unit cell. Identification of crystal axes was made optically and checked by X-ray diffraction. Deuterated crystals in which the polar hydrogens of glycine were exchanged for deuterium were grown from heavy water solutions. A single crystal was mounted on the spectrometer sample holder on a quartz fiber and irradiated on a liquid nitrogen bath. The exposure amounted to $1-3 \times 10^6$ roentgens from a 250-kev X-ray therapy machine. A crystal was then transferred, allowing as little warm-up as possible, to the refrigerated cavity of an esr spectrometer and allowed to warm at the rate of approximately 2°K/min. At any stage of the warming, the crystal could be recooled without affecting the character of the spectrum, although the amount of absorption increased, of course, inversely as the absolute temperature. Having determined at what temperatures spectral changes occur, an alternate procedure was to carry out the warming in a separate dewar and subsequently observe the spectra at 4.2°K. The spectrometer operated at a microwave frequency of 24.0 Gc using superheterodyne detection.

Results

At least three distinct esr spectra can be distinguished as crystals of glycine are allowed to warm following irradiation at liquid nitrogen temperature. There is the low-temperature spectrum which is probably due to ionic species, an intermediate spectrum which is the subject of this report, and the final spectrum which

has been reported previously.[4] A deuterated single crystal (polar hydrogens exchanged) irradiated at 77°K, warmed to 165°K, and observed at 4.2°K yields the spectra shown in Figure 1. The direction cosines of the applied magnetic field for each spectrum are given with respect to axes a, b, and c' fixed in the crystal, where c' is orthogonal to the crystalline axes a and b. The spectra of Figure 1 were recorded for field directions either parallel or perpendicular to the b axis, since for this condition all four molecules in the unit cell are equivalently oriented with respect to the field.

The spectra are attributed to a free radical formed from glycine by the removal of the amino group, either Ia or Ib. In either form the unpaired electron is expected to be localized primarily on the α-carbon atom in a $2p\pi$ orbital, and the bonding about the α-carbon atom should be planar. The hyperfine structure in the spectra of Figure 1 arises from magnetic interactions between the unpaired electron and the methylene protons. It is evident that the spectra are complex and that the hyperfine lines are of unequal intensity. The origin of this complexity is the fact that "forbidden" as well as allowed transitions contribute to the spectra. Allowed transitions are those in which only the magnetic quantum number associated with the spin of the electron changes. Forbidden transitions are those in which the magnetic quantum number of one or both protons also changes.

Ia Ib

The transition probabilities for electron spin resonance have been worked out by McConnell, *et al.*,[5] for the free radical COOH–CH–COOH, which is produced in malonic acid by X-irradiation. It is only necessary to generalize their results to include two interacting protons. The Hamiltonian for an electron and two interacting nuclear spins in the presence of a magnetic field is given by

$$\mathcal{H} = \beta_0 \bar{S}\cdot\hat{g}\cdot\bar{H} - g_n\beta_n\sum_{i=1,2}\bar{I}_i\cdot\bar{H} + \sum_{i=1,2}\bar{S}\cdot\hat{T}_i\cdot\bar{I}_i \qquad (1)$$

where β_0 is the Bohr magneton, $\bar{S}$ is the electron spin, $\hat{g}$ is the spectroscopic splitting tensor, $\bar{H}$ is the applied magnetic field, g_n is the nuclear g factor, β_n is the nuclear Bohr magneton, and $\bar{I}_i$ is the spin of the ith proton. The tensors, $\hat{T}_i$, describe the hyperfine interaction between the unpaired electron and the protons. If the components of $\bar{S}$ perpendicular to $\bar{H}$ are ignored, which is a good approximation, the energy levels of the spin system described by (1) are given by

$$E = \beta_0 g H S_H - g_n\beta_n\sum_{i=1,2} I_{ih}|\bar{h}_i| \qquad (2)$$

where g is the observed g value, S_H is the component of $\bar{S}$ along $\bar{H}$, and I_{ih} is the component of $\bar{I}_i$ along $\bar{h}_i$, where $\bar{h}_i$ is defined by the equation

$$\bar{h}_i = \bar{H} - S_H[\bar{u}_i A\alpha_i + \bar{v}_i B\beta_i + \bar{w}_i C\gamma_i] \qquad (3)$$

In (3), A, B, and C are the principal values of the hyperfine tensor, $\hat{T}_i$. While the principal values are expected to be the same for both hyperfine tensors, the directions of the principal axes are, of course, different. The directions of the two sets of principal axes are denoted by sets of unit vectors $\bar{u}_i$, $\bar{v}_i$, and $\bar{w}_i$, corresponding to A, B, and C, respectively. Direction cosines of the applied field with respect to these axes are indicated by α_i, β_i, and γ_i, respectively. Each component of spin, S_H, I_{1h}, and I_{2h}, in (2) may take the value $\pm 1/2$. The sixteen electronic transitions between levels of (2) are listed below in terms of $2\Delta Hg\beta_0/g_n\beta_n$, where ΔH is the displacement in gauss of the corresponding hyperfine line from the center of the absorption pattern. The vectors $\bar{h}_i(+)$ and $\bar{h}_i(-)$ are the values of $\bar{h}_i$ corresponding to S_H equal to $1/2$ and $-1/2$, respectively. The relative probabilities of the transitions are given as a function of the angle, ϵ_i, between the vectors $\bar{h}_i(+)$ and $\bar{h}_i(-)$ (see Table I).

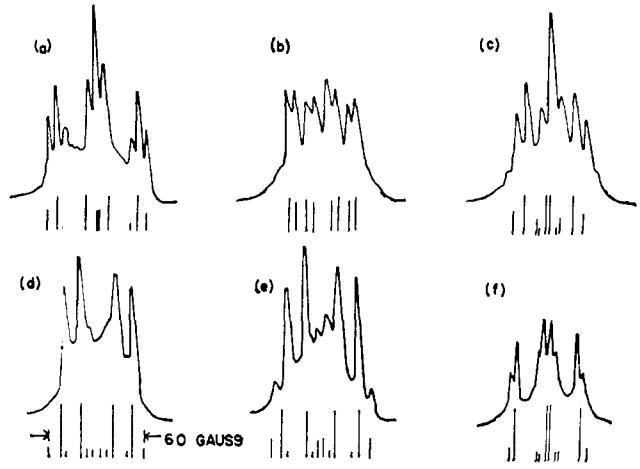

Figure 1. Esr absorption spectra for various orientations of a crystal of ND_3^+–CH_2COO^- irradiated at 77°K, warmed to 165°K, and measured at 4.2°K. Vertical lines show position and relative intensities of calculated transitions. Calculated transitions having a probability $<1/80$ the total transition probability are omitted. Direction cosines of the applied field with respect to axes a, b, and c' were as follows: (a) 0, 0, 1; (b) $\sqrt{2}/2$, 0, $\sqrt{2}/2$; (c) 0.966, 0, 0.259; (d) $\sqrt{3}/2$, 0, $-1/2$; (e) $\sqrt{2}/2$, 0, $-\sqrt{2}/2$; (f) 0, 1, 0.

Table I

$2\Delta Hg\beta_0/g_n\beta_n$	Probability
$\pm\lvert h_1(+)\rvert \pm\lvert h_1(-)\rvert \pm\lvert h_2(+)\rvert \pm\lvert h_2(-)\rvert$	$1/16 \sin^2 \epsilon_1/2 \sin^2 \epsilon_2/2$
$\pm\lvert h_1(+)\rvert \pm\lvert h_1(-)\rvert \pm\lvert h_2(+)\rvert \mp\lvert h_2(-)\rvert$	$1/16 \sin^2 \epsilon_1/2 \cos^2 \epsilon_2/2$
$\pm\lvert h_1(+)\rvert \pm\lvert h_1(-)\rvert \mp\lvert h_2(+)\rvert \pm\lvert h_2(-)\rvert$	$1/16 \sin^2 \epsilon_1/2 \cos^2 \epsilon_2/2$
$\pm\lvert h_1(+)\rvert \pm\lvert h_1(-)\rvert \mp\lvert h_2(+)\rvert \mp\lvert h_2(-)\rvert$	$1/16 \sin^2 \epsilon_1/2 \sin^2 \epsilon_2/2$
$\pm\lvert h_1(+)\rvert \mp\lvert h_1(-)\rvert \pm\lvert h_2(+)\rvert \pm\lvert h_2(-)\rvert$	$1/16 \cos^2 \epsilon_1/2 \sin^2 \epsilon_2/2$
$\pm\lvert h_1(+)\rvert \mp\lvert h_1(-)\rvert \pm\lvert h_2(+)\rvert \mp\lvert h_2(-)\rvert$	$1/16 \cos^2 \epsilon_1/2 \cos^2 \epsilon_2/2$
$\pm\lvert h_1(+)\rvert \mp\lvert h_1(-)\rvert \mp\lvert h_2(+)\rvert \pm\lvert h_2(-)\rvert$	$1/16 \cos^2 \epsilon_1/2 \cos^2 \epsilon_2/2$
$\pm\lvert h_1(+)\rvert \mp\lvert h_1(-)\rvert \mp\lvert h_2(+)\rvert \mp\lvert h_2(-)\rvert$	$1/16 \cos^2 \epsilon_1/2 \sin^2 \epsilon_2/2$

In order to calculate the hyperfine splittings and transition probabilities, it is necessary to know the orientation of the free radical (I) within the crystal. It is reasonable to suppose that the planes defined by the trigonal bonding about each carbon atom are, in fact, coplanar. This would allow the unpaired electron to conjugate with the carboxyl group. Hence, the free radical should be entirely planar. Since the carboxyl group is relatively more bulky and held in place by hydrogen bonding, one expects the free radical to lie in the plane defined by the carboxyl group of the

(5) H. M. McConnell, C. Heller, T. Cole, and R. W. Fessenden, *J. Am. Chem. Soc.*, 82, 766 (1960).

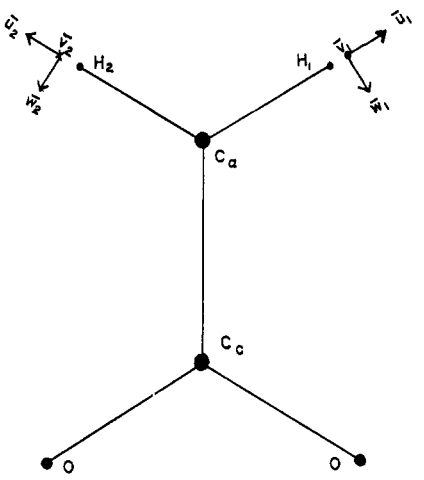

Figure 2. Proposed structure of the free radical showing directions of principal axes for hyperfine interactions.

undamaged molecule. Also, the direction of the C_α–C_c bond should remain virtually unchanged. Based on these assumptions, the orientation of the free radical relative to the crystalline axes can be calculated from the structure of glycine as determined by Marsh.[6] The directions of the principal axes, $\bar{u}_i$, $\bar{v}_i$, and $\bar{w}_i$, corresponding to minimum, intermediate, and maximum hyperfine splitting are parallel to the C_α–H_i bond, perpendicular to the plane of the molecule, and orthogonal to these directions, respectively, as shown in Figure 2. The direction cosines of the unit vectors were calculated relative to *a*, *b*, and *c'*. The results are given in Table II. The values of *A*, *B*, and *C* used in these calculations are those measured by McConnell, *et al.*,[5] in irradiated single crystals of malonic acid for the radical COOH-CH-COOH: $A = 29$, $B = 61$, and $C = 91$ Mc.

Table II. The Direction Cosines of the Principal Axes for the Hyperfine Tensors Calculated from the Data Given by Marsh[6] for a Reference Molecule

		a	*b*	*c'*
H_1	$\bar{u}_1$	−0.631	0.299	−0.715
	$\bar{v}_1$	0.191	0.955	0.227
	$\bar{w}_1$	−0.753	−0.011	0.659
H_2	$\bar{u}_2$	0.968	−0.141	−0.213
	$\bar{v}_2$	0.191	0.955	0.227
	$\bar{w}_2$	0.170	−0.265	0.949

The calculated hyperfine splittings and their relative intensities for various crystal orientations are shown in Figure 1 by vertical lines. The agreement between experimental and calculated results leaves no doubt that I is, in fact, the free radical being observed.

For completeness, the principal values and direction cosines of the principal axes of the *g* tensor for this absorption are given in Table III. The direction corresponding approximately to free spin is, as expected,[7] essentially perpendicular to the plane of the carboxyl group of the undamaged molecule.

(6) R. E. Marsh, *Acta Cryst.*, **11**, 654 (1958).
(7) W. M. McConnell and R. E. Robertson, *J. Phys. Chem.*, **61**, 1018 (1957).

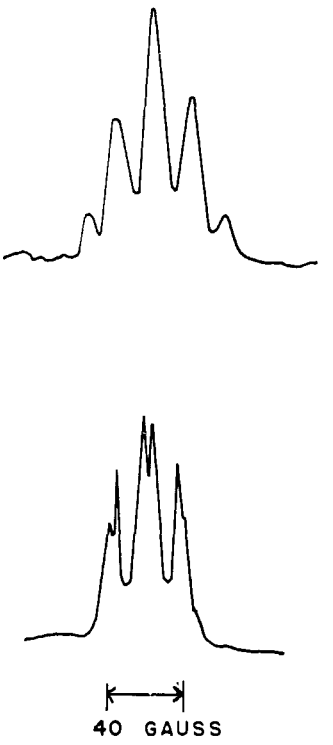

Figure 3. (a) Esr absorption spectrum for orientation (0, 1, 0) of a crystal of NH_3^+–CH_2COO^- irradiated at 77 °K, warmed to 165 °K, and measured at 4.2 °K. (b) Esr absorption spectrum of a crystal of ND_3^+–CH_2–COO^- for same conditions as (a).

The absorption spectra described above are essentially the same in normal and deuterated crystals, except that the hyperfine structure in the latter is better resolved. In normal crystals, additional outlying peaks can be observed for some crystal orientations (see Figure 3). Further studies of this absorption using isotopically labeled glycine are planned.

Table III. The Experimentally Determined Principal Values and Direction Cosines of the Principal Axes of the *g* Tensor for the Spectra Shown in Figure 1

	a	*b*	*c'*
2.0025	0.28	0.92	0
2.0038	0	0	1
2.0044	−0.92	0.28	0

Summary and Conclusions

Free-radical formation was examined in single crystals of glycine irradiated at low temperature. Using a controlled warming procedure, an intermediate phase of the radiation damage process was stabilized. From esr measurements, it was determined that the principal intermediate free radical results from cleavage of the C–N bond of glycine.

This result is consistent with the results obtained in the related amino acids alanine[8] and α-aminoisobutyric acid.[9] The final free radicals produced by X-irradiation in these amino acids are known to result exclusively

(8) I. Miyagawa and W. Gordy, *J. Chem. Phys.*, **32**, 255 (1960).
(9) H. C. Box and H. G. Freund, *Nucleonics*, **17**, 66 (1959); A. Horsfield, J. R. Morton, and D. H. Whiffen, *Trans. Faraday Soc.*, **57**, 1657 (1961).

from rupture of the C–N bond. Mechanisms by which the C–N bond may be broken have been discussed elsewhere.[10] Whereas the free radicals produced in alanine and α-aminoisobutyric acid by C–N bond breakage are stable at room temperature, those produced in glycine apparently are not. Considerable alteration in the esr spectra occurs at room temperature. Interpretation of the final spectra appears still to be a matter of lively controversy.[4]

Perhaps the most significant result of this research is to show that esr studies of single crystals at controlled temperatures, after irradiation at low temperature, offer considerable promise for following radiation damage processes.

(10) H. C. Box and H. G. Freund, to be published.

Solvent Mass Transfer across Ion-Exchange Membranes

A. S. Tombalakian,[1] M. Worsley, and W. F. Graydon

Contribution from the Department of Chemical Engineering and Applied Chemistry, University of Toronto, Toronto, Ontario, Canada. *Received August 31, 1965*

Abstract: A study of water diffusion across polystyrenesulfonic acid ion-exchange membranes, induced by osmotic pressure and cation diffusion potentials, has been made. The experimental results have been interpreted in terms of viscous interactions within the membrane during the transport process, between the ion and water, and between the water and membrane pore wall. Equations have been derived which relate solvent and ion transport rates with the viscous interactions within the membrane. These relationships were used to estimate friction coefficients for the interchange processes. The dependence of the ion–water interaction coefficient on inorganic and organic counter-ion diameter was determined.

Previous determinations of water transport across polystyrenesulfonic acid ion-exchange membranes by electroosmosis and ion interchange have been reported.[2–4] The results of measurements of water transport across similar membranes by osmosis (with solutions of HCl, KCl, NaCl, LiCl, $(CH_3)_4NCl$, and $(C_2H_5)_4NCl$ in the concentration range 0.1 to 1.0 *M*) and counter-diffusion of univalent inorganic and organic cations are given in this report. The results are consistent with theoretical considerations[5] of solvent transport phenomena through ion-exchange membranes. The dependence of solvent transport on membrane properties and the interchanging ion species has been determined.

Experimental Section

(A) Membranes. The membranes were prepared by the bulk copolymerization of the methyl and *n*-propyl esters of *p*-styrenesulfonic acid with styrene, divinylbenzene, and benzoyl peroxide as catalyst and subsequent hydrolysis in 5% caustic soda solution to produce polystyrenesulfonic acid.[3,6,7]

The methods used for the determination of membrane moisture content, exchange capacity, and thickness have been described previously.[6] In Table I are given the characteristics of the membranes and the membrane moisture contents in various ionic forms in contact with pure water at 25°.

(B) Solvent and Cation Transfer. A two-compartment Lucite cell was used to measure the rates of solvent and cation transfer. The compartments, each with a volume of 35 ml, were separated by a membrane with an area of 3.14 cm². The capillary tubes fitted into the cell were each 0.0856 cm in diameter. At the time of filling the cell, the solutions were adjusted to about the same level in both capillary tubes and the heights were measured using a cathetometer. After 1 hr the changes in the heights of the solutions were observed and the contents of the compartments were analyzed by titration. The procedure was repeated with fresh solutions until constant flux was obtained. The data reported here are average values for four individual measurements. All measurements were taken at 25 ± 0.1° with the solutions at rest in the cell. These data were used to calculate solvent transfer rates.

Results and Discussion

The osmotic flow rates are given in Table II. These measurements were made using various solutions of hydrochloric acid, potassium chloride, sodium chloride, lithium chloride, tetramethylammonium chloride, and tetraethylammonium chloride. The results were calculated from the experimental data using the relationship

$$J = \frac{(\Delta V)L}{tA} \qquad (1)$$

where J is the solvent flow rate in ml/cm hr; (ΔV) is the volume change in ml in t hr; L is the membrane thickness, 0.1334 cm; and A is the membrane cross section, 3.14 cm². Graphical representation of the increase of osmotic flow rate with increasing osmotic potential difference gave linear plots. The slopes of the straight lines correspond to osmotic permeability coefficients for the membrane in the given ionic forms. The observed values of the osmotic permeability coefficients are given in Table II. It may be noted that the osmotic permeabilities of the membrane in the various ionic forms decrease in the order hydrogen, potassium, sodium, lithium, tetramethylammonium, and tetraethylammonium, although the radius of the hydrated

(1) Department of Chemistry and Engineering, Laurentian University of Sudbury, Sudbury, Ontario, Canada.
(2) R. J. Stewart and W. F. Graydon, *J. Phys. Chem.*, **61**, 164 (1957).
(3) A. S. Tombalakian, H. J. Barton, and W. F. Graydon, *ibid.*, **66**, 1006 (1962).
(4) A. S. Tombalakian, C. Y. Yeh, and W. F. Graydon, *Can. J. Chem. Eng.*, **42**, 61 (1964).
(5) R. Schlögl and U. Schödel, *Z. Phyzik. Chem.* (Frankfurt), **5**, 372 (1955).
(6) W. F. Graydon and R. J. Stewart, *J. Phys. Chem.*, **59**, 86 (1955).
(7) W. F. Graydon, U. S. Patent 2,877,191 (March 10, 1959).